Online PET Reconstruction From List-Mode Data

Colas Schretter

***Abstract*—This work proposes an alternative to ordered subsets to improve the convergence speed of list-mode expectation-maximization image reconstruction algorithms. Instead of subdividing the input data into non-overlapping subsets, the stream of measured coincidence events is immediately processed online. The reconstruction algorithm maintains a sliding window covering the events that contribute to the current image estimate. The image is seamlessly updated by adding a new contribution for the next event read from the list-mode and possibly subtracting old contributions from a batch of events that leave the window. This incremental event-by-event estimation method can reconstruct a dynamic image sequence in real-time during data acquisition. If the reconstructed object is static, the width of the sliding window can be expanded during the reconstruction process to balance between early estimation and global convergence behaviors. Encouraging results are shown on image reconstructions from a simulated static phantom and from a clinical dataset of a dynamic cardiac perfusion study.**

***Index Terms*—Positron emission tomography, list-mode, maximum likelihood, expectation-maximization.**

I. Introduction

ORDERED SUBSETS (OS) have been used for long in emission tomography to improve the convergence speed of statistical image reconstruction algorithms based on the expectation-maximization (EM) framework [1]. In the popular OSEM method [2], an early image is estimated by considering only a small subset of the complete input data. Each successive sub-iteration produces a new result by using the latest image estimate and the next subset of data. In positron emission tomography (PET), the raw input data is a list of coincidence events measured by a ring of high energy photon detectors.

A drawback of reconstruction methods based on OS is that they are not in general convergent since the current image is built from a limited view of the complete data only. Fortunately, globally convergent variants that consider the full dataset have been developed. In the complete data ordered subset expectation-maximization (COSEM) algorithm [3], the best image estimate so far is equivalent to the sum of previous images computed by the classical OSEM algorithm.

An extension of COSEM, called ECOSEM [4], combines OSEM and COSEM. OSEM is used at early stage of the reconstruction process then COSEM is used to polish the image at the end of the run. The adaptation of OSEM from sinogram to list-mode by Reader *et al.* [5] produced impressive results. COSEM and ECOSEM have been adapted to list-mode by Khurd *et al.* [6] and Rahmim *et al.* [7], respectively. Faster event-by-event (EBE) variants of the list-mode OSEM and COSEM methods were introduced in a previous work [8].

The author was with the TEP/Cyclotron Biomédical, Hôpital Erasme, Université libre de Bruxelles (ULB), Brussels, Belgium (e-mail: cschrett@ulb.ac.be). He is now with Philips Research Europe, Aachen, Germany with financial support from the Marie Curie program of the European Commission under contract MEST-CT-2005-020424.

This paper introduces an alternative online reconstruction algorithm that does not rely on ordered subsets. Instead, the current image estimate is incrementally updated event-by-event. This approach improves convergence speed by directly using the new statistical information of each processed event. For static image reconstruction, the list of events can be read in a cyclic way such that the file is implicitly reset to return the very first event whenever the end of the list-mode is reached. This never-ending data stream model deprecates the concept of iteration over a dataset.

The next section introduces the sliding window expectation-maximization (SWEM) method for online image reconstruction from list-mode PET data. This new method is based on the incremental EM algorithm first proposed by Titterington in 1984 [9] and popularized by the seminal paper of Neal and Hinton [10]. The new reconstruction algorithm is driven by three intuitive parameters: the allowed budget of memory, the initial window width, and a window expansion factor.

II. SWEM

The rationale of the SWEM image reconstruction algorithm is the maintenance of an estimate of the maximum-likelihood solution that depends only on the most recent events read from a list-mode data instance. To achieve this goal, two algorithmic building blocks are needed. First, an operator that updates the current image for any measured coincidence event must be defined. This update have to increase the likelihood of the current image estimate. Second, incremental image updates from previous events must be archived for future subtraction. The most precise bookkeeping mechanism should be able to remember previous image modifications for each event. However, experiments demonstrate that such a fine storage granularity is not mandatory.

The SWEM algorithm is shown graphically in Fig. 1 and is parametrized by the number s of memory pages that select the granularity of the bookkeeping storage, the initial width w of the sliding window, and the window expansion factor $\delta \geq 1$ that drives a trade-off between early estimation and global convergence. The initial window width w can be set to the typical size of a OSEM subset. The number s of pages should be maximized in order to fit available memory resources. The window expansion factor δ drives the geometrical progression of page capacities.

The input dataset is denoted by N and the subscripts i select a particular event $i \in N$. The set of image elements to be estimated is denoted by M and the subscripts j select a particular image element $j \in M$. A set of indexed images β^p, $p \geq 1$ is considered available as memory pages. For the experiments, the image is initialized with an initialization constant $\varepsilon = 1$ such that $\lambda_j \leftarrow \varepsilon$, $\forall j \in M$. The initial image

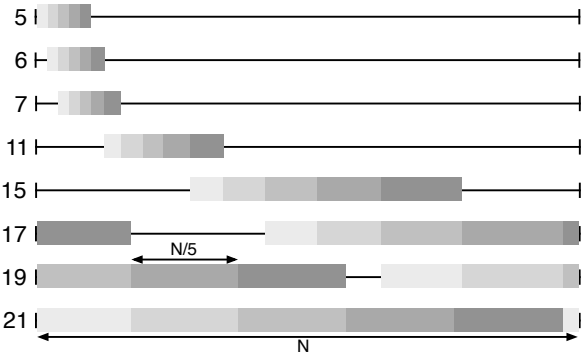

Figure 1. Graphical representation of the pagination-based bookkeeping mechanism of the SWEM algorithm. Different shades of gray delimit the splitting of the window in $s = 5$ non-overlapping pages. The width and position of each page are shown for some successive steps of the reconstruction process. The number of already processed pages is noted in front of each line while N equals the size of the whole data stream. An expansion factor $\delta = 1.25$ is chosen to increase progressively the sliding window width w. SWEM reach global convergence when $w = N$. In this example, the pages stop to expand once the maximum limit of N/s is reached.

must also be spread among the first bookkeeping pages, hence $\beta_j^p \leftarrow \varepsilon/s$, $\forall j \in M, 1 \leq p \leq s$.

The number of events that belongs to the page of index $p \geq 1$ is denoted by g^p. The initial size of the first pages are initialized accordingly to $g^p = w/s$, $1 \leq p \leq s$ and a variable p of the current page starts at $p = s + 1$. The next sections explain the three core principles that define the SWEM algorithm: incremental image update, paginated bookkeeping, and geometrical window expansion.

A. Event-by-Event Image Update

Event-by-event reconstruction algorithms adopt the incremental image update principle of COSEM. The COSEM method is proven to be convergent for any number of subsets and the convergence rate increases with the number of subsets [3]. The case of singleton subsets is therefore of special interest. With one event per subset, COSEM can be simplified to a direct incremental update followed by the subtraction of the previous image contributions for this event.

While the classical ordered subsets techniques have process all events of the current subset before exploiting their statistics, event-by-event image updates directly exploit statistical information from new events as soon as they are processed because the current image is used to weight backprojections along the line of response (LOR) of each event. For an event $i \in N$, the current image estimate λ is updated with

$$\lambda_j \leftarrow \lambda_j + \frac{A_{ij}\lambda_j}{a_i s_j \sum_{k \in M} A_{ik}\lambda_k}, \forall j \in M. \quad (1)$$

The element of the system matrix A_{ij} is equal to the probability than an annihilation occurring in image element $j \in M$ is detected along the LOR associated to event $i \in N$. The values of A are computed on-the-fly by a fast tube of response ray-tracer developed in a previous work [11].

The sensitivity correction factors s_j are equal to the ratio of annihilations occurring in image element $j \in M$ and detected by the PET scanner on the total number annihilations. These factors are proportional to the solid-angle that the detector edge subtends at the center of the voxels and can be precomputed for each image element using i.e. a semi-analytical method presented earlier [8].

The attenuation factors a_i are equal to the probability that the two collinear photons are not absorbed during their flight along the LOR of the event $i \in N$ whose length in centimeter equals l_i. According to Beer's law, this probability can be approximated by

$$a_i = \exp\left(-l_i \sum_{k \in M} A_{ik}\mu_k\right), \quad (2)$$

where μ is a linear attenuation image segmented into air, water, and lung materials. Attenuation factors per cm at 511 keV are stored for each voxel of the attenuation image.

Randoms are corrected according to the advices of Rahmim *et al.* [7] by subtraction of delayed events, while ensuring a definite positive image. For each event read from the input dataset, the current image is modified online by the incremental image update in (1). Only voxels straddling the LOR of the event will be modified. This key property makes it feasible to implement fast event-wise reconstruction methods because the ray-tracing algorithm can access only the relevant elements in both the emission and the attenuation images.

B. Bookkeeping Image Updates

The most straightforward way to remember previous modifications of the current emission image is simply storing the whole history of modifications for each image element. Remark that for each event, only the voxels along its associated LOR are modified and therefore only a short list of pairs containing an image bin identifier and the associated increment can be stored. Unfortunately, for a realistic input dataset counting several tens of millions of events and a detailed image definition, the amount of information to store is impractical.

To reduce the required memory resources, the processing of each event is nested in an outer loop that store in memory the accumulation of a batch of consecutive image updates. Before processing the events that will belong to the page β^p, the current image is first saved:

$$\beta_j^p \leftarrow \lambda_j, \forall j \in M. \quad (3)$$

After processing the $\lfloor g^p \rfloor$ next events with (1), the total of incremental updates can be retrieved by simple image difference:

$$\beta_j^p \leftarrow \lambda_j - \beta_j^p, \forall j \in M. \quad (4)$$

Once the page has been stored, the next page is considered by incrementing p and contributions of the oldest page β^{p-s} are removed from the current image:

$$\lambda_j \leftarrow \lambda_j - \beta_j^{p-s}, \forall j \in M. \quad (5)$$

The pagination technique trades storage granularity with storage capacity. Given a budget memory resources, the

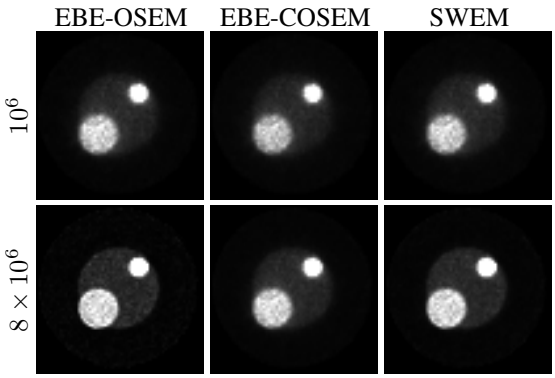

Figure 2. Reconstruction results of the numerical phantom. Each row contains the image estimates after processing 10^6 and 8×10^6 events, respectively. EBE-OSEM uses 16 subsets and is equivalent to SWEM with $s = 1$, $\delta = 1$ and $w = 5 \times 10^5$. EBE-COSEM corresponds to SWEM with $s = 16$, $\delta = 1$ and $w = 8 \times 10^6$. The third column shows results of SWEM with $s = 4$, $\delta = 1.1$ and an initial window width $w = 5 \times 10^5$.

memory is segmented into several pages of the size of the output image. Then incremental updates corresponding to several events are accumulated into the pages. In practical implementations, the pages will be stored in a cyclic buffer of size s in order to limit memory requirements.

C. Window Expansion

Page capacities g^p are counted in number of events and depend geometrically on the previous page such that $g^p = \delta g^{p-1}$. Therefore, the window width is continuously expanded if $\delta > 1$. Stopping the reconstruction when the window covers all the available data ensure that the SWEM algorithm reached a convergent behavior. It is easy to evaluate the value of δ given the initial window width w, a number events to process N, and the amount of available pages p. Indeed, the geometrical progression of the page size can stops when $g^p = N/s$ and since $g^p = (w/s)\,\delta^{p-s}$, then $\delta = \sqrt[p-s]{N/w}$.

For some choices of the parameters w, s, and δ, it is easy to see that EBE-OSEM and EBE-COSEM algorithms [8] are special cases of SWEM. If $\delta = 1$, then the width of the window will never increase and thus the capacity of each page stays constant. Moreover, if one chooses $w = N/k$ and $s = 1$, then the technique yields EBE-OSEM with k subsets because only a fraction of the events contributes to the estimation. On the other hand, if one chooses $w = N$, then the whole dataset is covered by the window and the algorithm reduces to the globally convergent EBE-COSEM method.

III. Results

Assessment of the SWEM method has been conducted from the reconstruction of a nested balls phantom defined by four uniform regions described in normalized coordinates as follows. Two balls of radius 0.25 and 0.125 are superposed over a ball of radius 0.5 centered at the origin. The densities of these three spheres are respectively 1, 4, and 8. A uniform background noise signal of density 0.1 has been modeled too with a sphere covering the whole field of view.

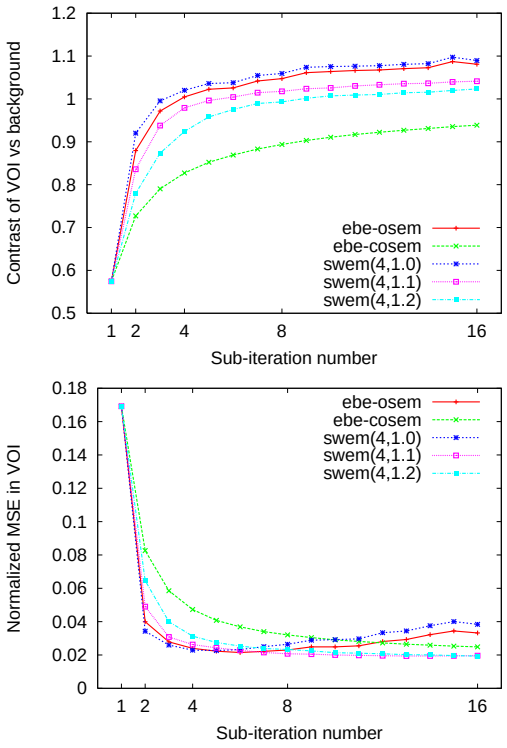

Figure 3. The contrast recovery coefficient and the normalized mean squared error (MSE) from the objective image are plotted for various values of the expansion factor $\delta \in \{1.0, 1.1, 1.2\}$ with a number of memory pages fixed to $s = 4$ for SWEM. The results of the EBE-OSEM and EBE-COSEM methods with 16 subsets are also shown for comparison. The sub-iteration numbers correspond to multiples of 5×10^5 events.

A list-mode dataset of 8 millions events has been generated by simulating the emission process. For each event, one ball is picked and an annihilation position inside the sphere and an emission direction is randomly sampled. From the radius and density of each ball, a discrete probability density function can be defined such that the probability of selecting a ball depends on its density and its volume.

Reconstruction results are shown in Fig. 2. Each reconstructed image is a matrix of 64^3 voxels but only the median transversal slice is shown. After processing one million events, we already observe that the EBE-OSEM and SWEM methods of the left and right columns produce sharper images compared to the EBE-COSEM method of the central column. The images of the second row correspond to the result after only one pass over the data.

Quantitative analysis of the reconstructed images is shown in terms of contrast recovery and mean squared error (MSE) from the objective emission image in Fig. 3. The visual contrast is defined as the ratio between the reconstructed mean activity in the small high activity ball (VOI) and the mean activity in a reference region inside the background. With an appropriate window expansion factor, SWEM prevents overfitting the data and provides a better result than OSEM.

Fig. 4 shows selected transversal slices of a dynamic image reconstruction from a clinical cardiac perfusion study. The data has been acquired during two minutes on a Philips Gemini PET/CT scanner. A bolus of N-13 ammonia tracer is injected

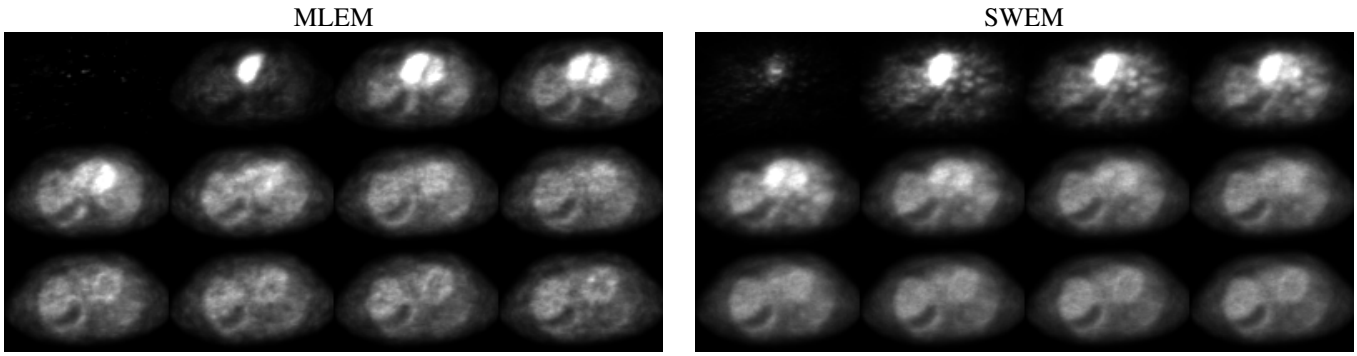

Figure 4. Slices from the dynamic images of a cardiac perfusion reconstructed by MLEM with 32 iterations and SWEM. A snapshot is shown every 10 seconds for the two first minutes of acquisition. However, since the SWEM method reconstructs a new image for each event, all the intermediate frames are available as well. For SWEM, the window width is adapted dynamically to cover events measured in the past 10 seconds.

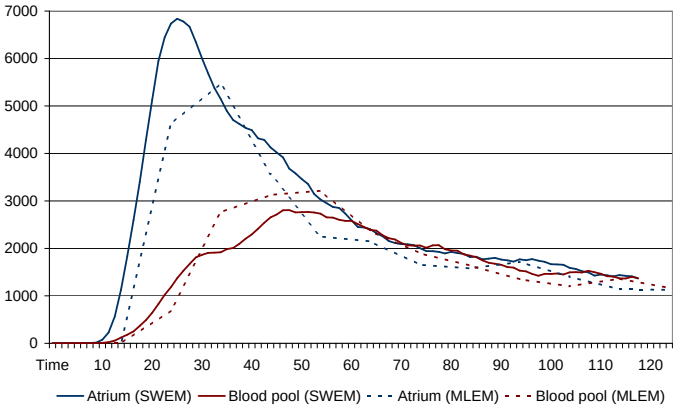

Figure 5. Time activity curves (TAC) measured at two voxels located in the right atrium and in the blood pool. The dotted path is a linear interpolation from frames that are independently reconstructed with MLEM. One frame is reconstructed every 10 seconds and therefore the resulting TACs lack temporal coherence. TACs estimated with SWEM tend to recover unambiguously the position and amplitude of peaks.

intravenously when the patient lies under the PET scanner. The tracer quickly enters the blood pool during the first few seconds of acquisition and then, passively diffuses into tissues. The left ventricular wall become visible at the end of the exam.

Fig. 5 plots two time activity curves (TAC) that have been sampled inside the right atrium and the left ventricle. In comparison to the reconstruction of independent frames with MLEM (32 iterations), the TACs estimated by the online SWEM method are smoother and exhibit a much more plausible physiological behavior. Moreover, the contrast between the two different activity curves is improved.

IV. Conclusion

This work presents SWEM: a general online image reconstruction method for PET list-mode data. The online approach based on event-by-event incremental updates allows direct improvement of the image by exploiting the new statistical information of events as soon as they are measured. The technique is explained by the concept of a sliding window covering the data elements contributing to the current image estimate. By expanding progressively the window width, the SWEM algorithm can smoothly balance between early estimation and global convergence behaviors.

Results from simulated phantom data have shown that a further increase in performance over event-by-event variants of the OSEM and COSEM algorithms is possible. Furthermore, a preliminary dynamic image reconstruction from clinical data demonstrates the potential of SWEM for improving image quality in comparison to the reconstruction of independent frames with MLEM. Further work on ground truth experiments is needed to evaluate quantitatively the potential accuracy of dynamic reconstruction with SWEM.

Acknowledgment

The author expresses his appreciation to Michel Defrise for his insights and discussions about image reconstruction. He would like to thank Ralph Brinks for early reviews of this work and Serge Goldman for granting financial support.

References

[1] A. P. Dempster, N. M. Laird, and D. B. Rubin, "Maximum likelihood from incomplete data via the EM algorithm," *J. Royal Stat. Soc.*, vol. 39, no. 1, pp. 1–38, 1977.

[2] H. M. Hudson and R. S. Larkin, "Accelerated image reconstruction using ordered subsets of projection data," *IEEE Trans. Medical Imaging*, vol. 13, no. 4, pp. 601–609, 1994.

[3] I.-T. Hsiao, A. Rangarajan, and G. Gindi, "A provably convergent OS-EM like reconstruction algorithm for emission tomography," *Proc. SPIE Medical Imaging*, vol. 4684, pp. 10–19, 2002.

[4] I.-T. Hsiao, A. Rangarajan, P. Khurd, and G. Gindi, "An accelerated convergent ordered subsets algorithm for emission tomography," *Physics in Medicine and Biology*, vol. 49, no. 11, pp. 2145–2156, 2004.

[5] A. J. Reader *et al.*, "One-pass list-mode EM algorithm for high resolution 3D PET image reconstruction into large arrays," *IEEE Trans. Nuclear Science*, vol. 49, no. 3, pp. 693–699, 2002.

[6] P. Khurd, I.-T. Hsiao, A. Rangarajan, and G. Gindi, "A globally convergent regularized ordered-subset algorithm for list-mode reconstruction," *IEEE Trans. Nuclear Science*, vol. 51, no. 6, pp. 719–725, 2004.

[7] A. Rahmim, J. C. Cheng, S. Blinder, M. L. Camborde, and V. Sossi, "Statistical list-mode image reconstruction for the high resolution research tomograph," *Physics in Medicine and Biology*, vol. 49, no. 8, pp. 4239–4258, 2004.

[8] C. Schretter, "Event-by-event image reconstruction from list-mode PET data," *IEEE Trans. Image Processing*, vol. 8, no. 1, pp. 117–124, 2009.

[9] D. M. Titterington, "Recursive parameter estimation using incomplete data," *J. Royal Stat. Soc.*, vol. 2, no. 46, pp. 257–267, 1984.

[10] R. M. Neal and G. E. Hinton, *A view of the EM algorithm that justifies incremental, sparse, and other variants*, pp. 355–368. Kluwer, Boston, MA, USA, 1998.

[11] C. Schretter, "A fast tube of response ray-tracer," *Medical Physics*, vol. 33, no. 12, pp. 4744–4748, 2006.